Monitoring microbial population dynamics at low densities

Thomas Julou,[1,a)] Nicolas Desprat,[1,2] David Bensimon,[1,3] and Vincent Croquette[1,b)]
[1]*Laboratoire de Physique Statistique de l'École Normale Supérieure, UMR8550, associé au CNRS et aux Universités Paris VI et Paris VII, 24 rue Lhomond, 75005 Paris, France*
[2]*Université Paris Diderot 75205 Paris Cedex 13, France*
[3]*Department of Chemistry and Biochemistry, University of California, Los Angeles, Los Angeles, California 90095, USA*

(Received 5 March 2012; accepted 3 June 2012; published online 11 July 2012)

We propose a new and simple method for the measurement of microbial concentrations in highly diluted cultures. This method is based on an analysis of the intensity fluctuations of light scattered by microbial cells under laser illumination. Two possible measurement strategies are identified and compared using simulations and measurements of the concentration of gold nanoparticles. Based on this comparison, we show that the concentration of *Escherichia coli* and *Saccharomyces cerevisiae* cultures can be easily measured *in situ* across a concentration range that spans five orders of magnitude. The lowest measurable concentration is three orders of magnitude (1000×) smaller than in current optical density measurements. We show further that this method can also be used to measure the concentration of fluorescent microbial cells. In practice, this new method is well suited to monitor the dynamics of population growth at early colonization of a liquid culture medium. The dynamic data thus obtained are particularly relevant for microbial ecology studies. © *2012 American Institute of Physics*. [http://dx.doi.org/10.1063/1.4729796]

I. INTRODUCTION

Microbial populations have become important model systems in ecology and evolution. Their fast growth rates compared to higher metazoans make them usable as a model to address a variety of topics such as population dynamics,[1–3] ecological interactions,[4] adaptation,[5] and differentiation.[6] The advantages and limitations of microbial experimental systems in ecological studies are discussed in detail in Jessup, Forde, and Bohannan.[7] Experimentally, it is difficult to monitor microbial growth at low population density. This is necessary in order to discriminate between different dynamic scenarios. The development of a microbial infection, for example, is highly dependent on the success of initial colonization. It is therefore particularly important to be able to characterize precisely the dynamics of an infection at its early stages when the pathogen population is sparse. Furthermore, an experimental system capable of discriminating between several cell types is also required in order to understand the growth of mixed populations in competition experiments or microbial differentiation dynamics during growth. Presently, microbial concentrations in liquid cultures are essentially measured in one of two ways − either by methods in which cells are sampled and counted individually, or by bulk photometric methods in which the average population is measured *in situ* in the growth environment. Although sample and count methods do offer good accuracy at low population densities, they have the downside that they are invasive. Conversely, bulk photometric methods are less invasive but are not reliable at low population densities.

A. Sample and count methods

Manual counting methods necessitate sampling during the microbial growth phase (several hours). These methods are thus time consuming and, at each time point, a sample needs to be taken out of the culture medium and either poured into an evaluation chamber or plated onto a petri dish after dilution. Using a microscope, microbial concentration can then be measured by counting the number of individual cells in a known volume.[8] This technique is not standardized as it requires the use of a microscope. On petri dishes, the concentration of living cells is measured as the number of colony forming units. This method is commonly used but is prone to several biases such as spatial growth inhibition between adjacent colonies, desiccation effects, and improper microbial separation during sample preparation.

Sophisticated apparatus such as Coulter counters or flow cytometers allow individual cells to be counted in an automated manner after culture sampling. The Coulter counter measures the variations of impedance due to the transit of particles through a small hole in a membrane separating two electrolyte solutions. This has been successfully used to measure low bacterial concentrations[9,10] and growth rates of small populations in low glucose concentration.[11] The flow cytometer measures the light scattered by individual cells flowing through a capillary: it is suitable for counting microbes and can be extended to the study of phenotypic traits using fluorescent markers.[12,13]

B. Bulk photometric methods

Microbial concentration can also be measured *in situ*, either from the amount of light scattered by the cells or from the attenuation of transmitted light passing through

a)thomas.julou@normalesup.org.
b)vincent.croquette@lps.ens.fr.

the culture chamber. The latter approach is widely used in laboratories and is called optical density (OD). The OD is defined as $-\log(I/I_0)$ where I and I_0 are the transmitted light intensities measured, respectively, through a sample and a blank solution of defined thickness. OD has been shown to measure biomass rather than the cell number.[14] This technique has been improved for samples of variable thickness[15] and for continuous measurements at 950 nm with real-time calibration.[16] However, this method remains unable to measure accurately bacterial population densities below 10^7 ml^{-1}. Indirect methods have been proposed to improve the precision at low concentrations based on repeated measurements.[17,18]

C. Recent developments

Another method of cell detection has recently been proposed, based on holographic microscopy. An interference image of the culture solution is used to reconstruct a three-dimensional image of the population.[19] This approach brings several improvements over existing techniques, in particular the position of each microbial cell can be determined precisely. However, the computation time required to reconstruct the image from the hologram (400 s below 10^5 ml^{-1}, more for higher concentrations) is limiting. In addition, this method cannot discriminate between different fluorescent properties of the individuals (when compared to flow cytometry, for instance).

This rapid overview, summarized in Table S1 of the supplementary material,[20] highlights that each of these different methods has certain limitations.

An ideal measurement method should provide data in real time and be accurate across a wide range of concentrations. It would also be minimally invasive, i.e., requiring no sampling and such that practical constraints (observation window, contact with the liquid, etc.) are minimized. Finally, it should also allow one the ability to distinguish between several microbial populations within the same culture on the basis of their fluorescence (generated, for example, via the expression of different fluorescent protein markers).

Here, we present a novel method for direct microbial concentration determination based on measurements of the fluctuations of the light scattered by microbes passing through a laser beam. Importantly, the method is non-invasive, accurate at low microbial concentrations (down to 10^4 ml^{-1}), and can be extended to determine concentrations of more than one microbial population.

II. MATERIAL AND METHODS

A. Setup description

The device underpinning our novel method features a spectroscopy cuvette in a custom-made temperature-controlled holder, illuminated with a focused 532 nm diode-pumped solid-state laser. Both the MGL-III-532 from CNI, Changchun, China and the GCL-050-L from Crystal Laser, Reno have been tested. At the focal point, the typical beam width (estimated as two standard deviations of the Gaussian light intensity profile) is 80 μm for the former and 120 μm for the latter. The total power is adjusted to ~5 mW. The laser beam is imaged orthogonally using a CCD camera (JAI, BM-141 GE) conjugated with the sample by a tube lens and a 10× infinity-corrected objective (Olympus PLN 10×) (Fig. 1).

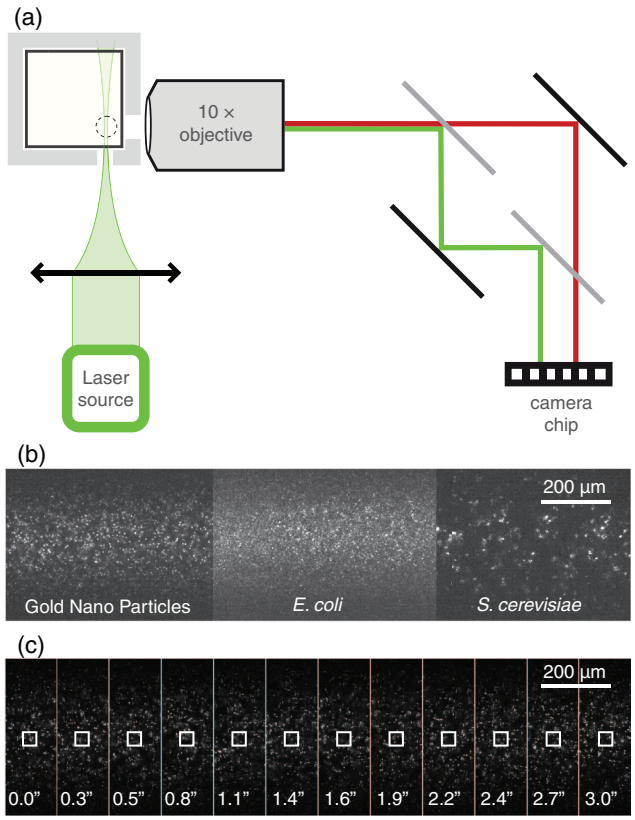

FIG. 1. Setup used for the new microbial concentration measurement method. (a) Schematic of the setup (bandpass filters, tube lens, and aperture diaphragm are not shown). In order to minimize aberrations, we use an infinity-corrected objective. Using a 50 mm tube lens with a 18 mm effective focal length objective (10×) yields approximately a 2.77× magnification. The dual view setup is used for Fluorescence Intensity Fluctuations (FIF) measurements only. (b) Typical scattered light picture obtained with GNPs (left, 7×10^7 ml^{-1} in water), *E. coli* cells (center, 10× dilution of an overnight culture in LB), *S. cerevisiae* cells (right, 10× dilution of an overnight culture in YNB supplemented with 80 mM glucose). Only the scattered light channel is shown. Contrast has been adjusted on each picture, thus darker background corresponds to higher signal-to-noise ratio. (c) Typical scattered light time lapse sequence obtained with 200 nm GNPs at 7×10^6 ml^{-1}. Acquisition frequency is 3.77 Hz and exposure time is 3.5 ms. A white box is added to help appreciate the fluctuations of intensity in a given area. Contrast has been adjusted to improve particle visibility. Scale bar is 200 μm (enhanced online) [URL: http://dx.doi.org/10.1063/1.4729796.1].

In order to stir the particles and homogenize the solution, a custom-made magnetic stirrer is included in the cuvette holder and remotely controlled by the acquisition software.

B. Image acquisition and real-time analysis

Pictures are acquired at low frequency (typically 3 Hz) and treated in real time using the following algorithm (Fig. 2(a)): (i) the current image background is corrected by subtracting a mean black image acquired using the same parameters but without illumination; (ii) the region of interest

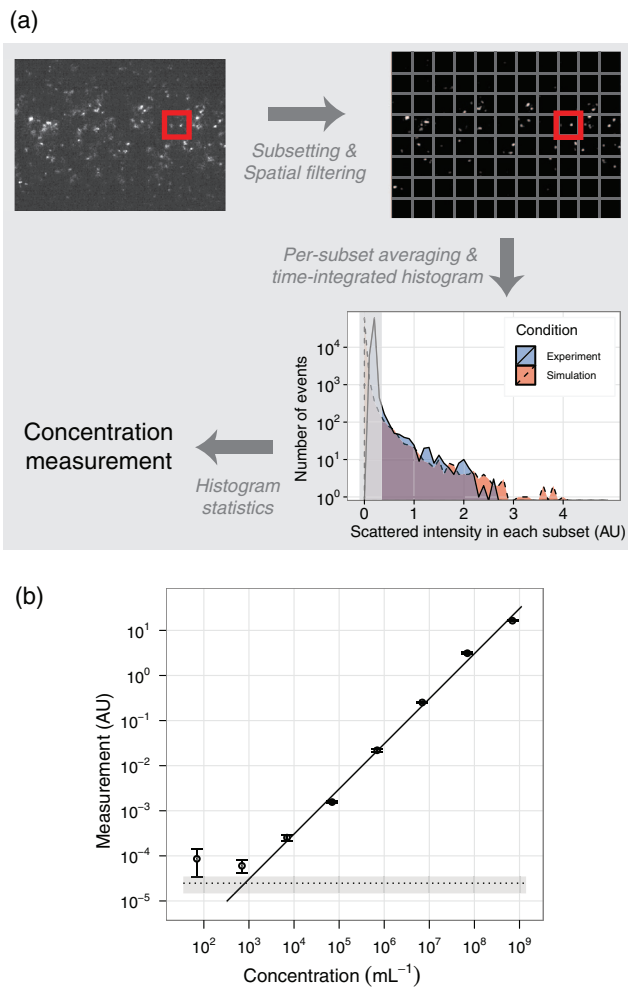

FIG. 2. Principle and (GNPs)-based validation of the measurement method. (a) Principle of data treatment workflow to estimate a concentration from a raw image (see Secs. II B and III A for details). The effect of the spatial bandpass filter is highlighted on a sample subpicture using a red box. The histogram of scattered light intensities shows the typical shapes obtained with GNPs at 7.0×10^4 ml^{-1} (60 s at 3.5 Hz) and with a simulation at the same concentration (200 frames). Intensities below the background level (greyed area) are not taken into account to compute the statistics. (b) Relationship between the absolute concentration and the estimation for serially diluted solutions of 200 nm GNPs. Points and error bars are mean and SEM (over 10 repeated 1 min-long measurements), respectively, dashed lines and greyed areas indicate the background level measured in water. The solid line shows a linear fit with slope fixed to 1; open symbols correspond to saturation and are not used in the fit.

($\sim$5 laser beam σ width) is split into 16×16 pixel^2 images with 2 pixel overlap on each edge; (iii) these small images are spatially bandpass filtered in order to remove the low frequency variations representing slow drift and the high frequency variations which are mainly noise; (iv) the scattered intensity I, defined as the root-mean-square of the intensity at the center of filtered images (to avoid treating overlapping area twice), is computed and stored in an accumulated histogram; (v) the concentration is computed from the histogram statistics (in the FIS method, it is computed as $\langle I \rangle^2/\sigma_I^2$; see Sec. III A for details) and can be stored during time for time-lapse acquisitions. Acquisition and data treatment are written in C, using a custom API and user interface; source code is available upon request. Further data analysis is performed with R, using ggplot2 for publication plots.

In calibration experiments, the signal is acquired over the course of 1 min for each measurement. In growth experiments, it is acquired during 3 min and the solution is stirred for 15 s (followed by a 25 s delay to allow the fluid to come to rest) between each measurement.

In calibration experiments with biological cultures, OD is measured at 600 nm using an Eppendorf Biophotometer.

C. Chemicals, strains, and media

A solution of 200 nm-wide gold nanoparticles (GNPs) (BBInternational, Cardiff, UK) serially diluted in milli-Q water is used to validate the method. Subsequent calibrations and growth experiments are run on the bacteria *Escherichia coli* MG1655 and the yeast *Saccharomyces cerevisiae* S288C. With *E. coli*, calibrations are performed using an overnight culture in Luria Bertani rich medium (LB) at 37 °C, resuspended and serially diluted in 10 mM magnesium sulfate. In growth experiments, bacteria are grown at 37 °C in M9 minimal medium supplemented with 0.4% glucose and 2 mM magnesium sulfate. With *S. cerevisiae*, calibrations are performed using an overnight culture in yeast nitrogen base (YNB) medium supplemented with 80 mM glucose at 30 °C, resuspended and serially diluted in 10 mM magnesium sulfate. In growth experiments, yeasts are preliminary grown overnight at 30 °C in YNB medium supplemented with 80 mM glucose.

During calibrations, the actual concentration is measured by plating a diluted solution of the overnight culture on LB-agar for *E. coli* and yeast peptone dextrose-agar for *S. cerevisiae*. The dilution factor is chosen so as to count 30–200 colonies per plate after growth at 37 °C for *E. coli* and 30 °C for *S. cerevisiae*.

Disposable cuvettes made from optical polystyrene with four clear sides (Kartell, Noviglio, Italy) are used in order to reduce sample pollution by dust as much as possible. All media and buffers are filtered using 0.2 μm disposable filters.

III. THEORY AND SIMULATIONS

This new method for detection of microbial concentration is based on measurements of the fluctuations of the light scattered by microbes passing through a laser beam. After image acquisition and real-time analysis, we record a time-integrated histogram of the intensity of the light scattered by the cells (see Sec. II B).

A. Measurement principle

Based on this distribution of intensities, two methods can be used to estimate the sample concentration. The first approach considers each microbial cell as a "particle." When the microbial concentration is low, the presence of a particle in the excitation volume is a rare event which follows a Poisson distribution. If λ is the mean number of particles (scattering events) in the observation volume during the observation

time, then the probability of observing no particles is $P(n=0) = e^{-\lambda}$. We can thus use the probability of no scattering event as an estimate for the mean number of particles in the scattering volume ($\lambda = -\ln(P(n=0))$). Since this method requires an estimate of the probability distribution of events $P(n)$, the acquisition time increases as the particle concentration gets lower. It is also not expected to work when the particle concentration is high and the probability of having no particles in the observation volume is therefore small.

The second method is based on an analysis of the fluctuations in the intensity of the scattered light (FIS). If there are n particles in the observation volume, the mean intensity of the light scattered in the observation volume over time will be proportional to $\langle I \rangle = nI$ (where I is the average intensity scattered by one particle), while the variance $\sigma_I^2 \propto nI^2$. Hence, the number of particles n is proportional to $\langle I \rangle^2/\sigma_I^2$ (a similar result is obtained for the number of scattering molecules in fluorescence correlation spectroscopy (FCS)). This technique is also related to fluorescence intensity distribution analysis.[21]

Finally, multiple light scattering (i.e., the fact that a photon is scattered by several particles before being detected) is likely to set the upper limit with both methods. Nonetheless, the single scattering regime has been shown to extend up to 10^8 ml^{-1} for bacterial cultures.[22] Consequently, multiple scattering will not perturbate our measurement at low and intermediate concentrations.

B. Simulations

In order to compare these two methods and to study the effects of various parameters on sampling errors and on saturation, pictures of light diffusion by particles in a Gaussian beam were simulated (see Fig. S1 caption of the supplementary material for details[20]) and analyzed using the same algorithm used to analyze the camera pictures.

These simulations show that the two methods can provide an accurate measurement over a wide range of concentrations (Fig. S1).[20] However, it is not possible to estimate the population density using the Poisson method when the number of particles in the observation volume is too large ($P(n=0) \to 0$) or too small ($P(n=0) \to 1$). This somewhat limits its dynamic range to a still very favorable four orders of magnitude in concentrations. The FIS method does not have these drawbacks, though its accuracy decreases at high concentrations (where the relative fluctuations are small and multiple scattering is likely to occur). At low concentrations, the FIS method achieves a better accuracy if the sampled volume is larger.

In this respect, the best strategy appears to be the FIS method with a large beam (large excitation volume). Hereafter, the results of both methods are shown in the case of GNPs (in supplementary material figures), but for all biological calibrations and applications only the FIS method was used.

IV. RESULTS

The method we propose is simple and does not require sophisticated equipment. This method is different from classical photometry measurements and is rather akin to FCS which has been used to estimate the concentration of fluorescent molecules. In practice, we record images of the light scattered by microbial cells (bacteria and yeast) as they pass through a laser beam illuminating their solution. To do so, we illuminate the sample solution with a focused laser beam. We image the light scattered by the cells perpendicular to the beam on a CCD camera. In these images, the microbes appear as bright dots (Figs. 1(b) and 5). The intensity of the dots (i.e., the intensity of the scattered light) decreases with the distance of the cell to the center of the Gaussian beam.

Images are analyzed in real time so as to compute the microbial concentration. Because of real-time analysis, we only record the time-integrated histogram of the intensity averaged on subregions of the original image after filtering (see Sec. II B). Typical distributions are shown for diluted solutions (GNP and simulation) (Fig. 2(a)). At low concentration, the rapid decrease of the histogram is in agreement with the shape of the intensity distribution of light scattered by particles passing through a Gaussian beam ($\propto 1/I$).

Based on this distribution of intensities, we use the FIS method to estimate the microbial concentration (see Sec. III A for details).

A. Validation using GNPs

Since microbes are variable in size, shape, and optical properties, GNPs are used to validate the approach and calibrate the setup. These gold particles were chosen as they produce a clean and strong scattered light signal (very similar to the signal from microbial cells). Using our approach, and analyzing the signal with both methods (Poisson or FIS), yields a concentration estimate for serially diluted solutions that exhibits (with both methods) a linear dependence on the actual concentration over five orders of magnitude (Fig. 2(b) and Fig. S2(a) of the supplementary material[20]). At very high dilution ($<2 \times 10^3$ ml^{-1}), the particulate background in the distilled water used is too large and generates a dilution independent scattering signal.

Above 10^5 ml^{-1}, the reproducibility of the data (defined as standard error of the mean (SEM) over 10 replicates) is better than 7% (Fig. S2(b)[20]). Below 10^5 ml^{-1}, the error between replicas increases, possibly due to slight variability in the dilution protocol.

At this point, several experimental caveats must be mentioned. First, the absolute value of the scattered intensity depends on several parameters (particle type, illumination intensity, exposure time, etc.). Consequently, the present method needs to be calibrated in order to get concentration measurements in units of particle per volume. Second, illumination conditions and exposure times must be adjusted for each type of particle in order to be able to use the full dynamic range of the camera (with saturation lower than 0.1%) while keeping exposure times short enough to acquire sharp particle images (less than 20 ms with our setup). The velocity of the particles not only constrains the exposure time but also the acquisition frequency which is chosen in order to be able to acquire independent images – this acquisition is typically run at 2 Hz–7 Hz.

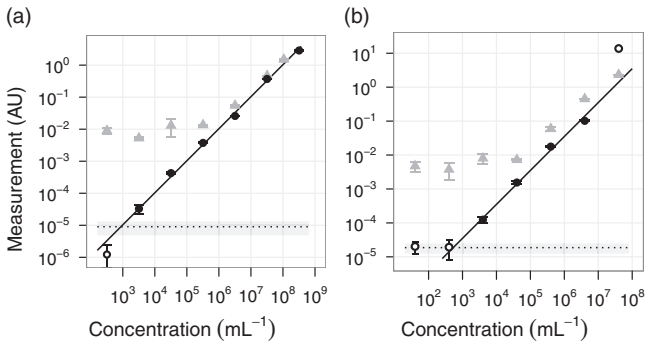

FIG. 3. Calibrations with bacteria *E. coli* MG1655 (a) and yeast *S. cerevisiae* S288C (b). Cell counting values are shown with black circles and OD values are plotted with grey triangles for comparison. Points and error bars are mean and SEM of ten repeated measurements (four in the case of OD), dashed lines and greyed areas indicate the background level measured with a magnesium sulfate solution. The solid lines show linear fits with slope fixed to 1; open symbols correspond to saturation and are not used in these fits.

B. Concentration measurement of microbial populations

We have tested our approach with measurement of the concentrations of different microbial species. Here, we report the results with two widely used model organisms: the bacteria *E. coli* and the unicellular eukaryote *S. cerevisiae*.

Using serial dilutions of a stationary phase culture of *E. coli*, we show that the population density measured by the FIS method yields an accurate and reproducible estimate for densities varying from 5×10^3 ml^{-1} to 5×10^8 ml^{-1} (Fig. 3(a)).

In comparison, OD measurements on the same samples are not reliable below 10^6 ml^{-1}. Consequently, our method, using a very simple setup, constitutes a 100-fold improvement on the lower detection limit of this standard method, with an extended dynamic range of almost five orders of magnitude.

Similarly, we show that estimation of the population density of *S. cerevisiae* is accurate and reproducible from 10^3 ml^{-1} to 10^8 ml^{-1} for a serially diluted stationary phase culture (Fig. 3(b)). Here too, the range of OD measurements is narrower, in particular at low concentrations since the OD lower limit stands at $\sim 5 \times 10^5$ ml^{-1}. Unexpectedly, the saturation at high concentrations is more pronounced than for GNPs or *E. coli*. In these latter cases, high concentrations are slightly underestimated which may be due to multiple scattering. With yeast, high concentrations ($>10^8$ ml^{-1}) are strongly overestimated which limits the relevance of our method for concentrated yeast cultures.

The results we have obtained are from cells of very different sizes (from 1 μm to 10 μm) and shapes (rod-shaped bacteria vs spherical to ellipsoidal yeast cells). Importantly, they show that the method we introduce in this paper is working not only with isotropic particles of homogeneous size but more generally across a wide range of optical objects.

C. Microbial growth monitoring

Using our setup, we have monitored the growth of *E. coli* populations starting from a very dilute state (<5000 ml^{-1}). In these conditions, the bacteria exhibit a lag phase, with little growth, followed by an exponential growth phase, and ending in a stationary phase where bacteria having exhausted the nutrients do not grow anymore (Fig. 4(a)). Our setup allows monitoring of the exponential growth phase over four orders of magnitude. As the initial dilution corresponds to ~ 5000 ml^{-1}, the long lag phase seen in the plot (at least 4 h) is likely to be due to a combination of biological lag (required for bacteria to switch on growth) and to the limited accuracy of our detection method at these low concentrations (below 10^4 ml^{-1}). The variability in the culture yield (assessed by the stationary phase variation in saturating population density) is likely to be due to variations in the availability of oxygen between replicates, a well-known effect when growing *E. coli* in M9 minimal medium.

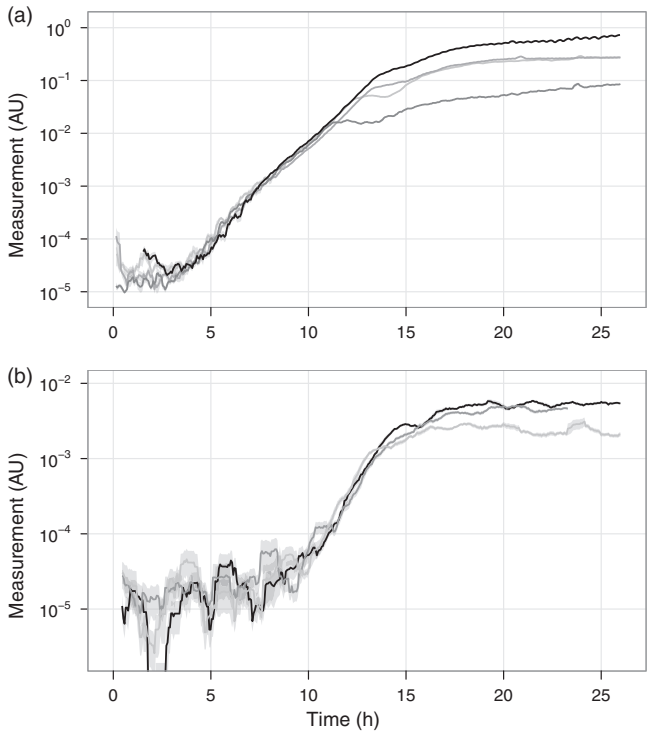

FIG. 4. Microbial growth monitoring. (a) Growth of bacteria *E. coli* MG1655 in M9 minimal medium supplemented with 0.4% glucose at 37 °C. Stationary phase culture are diluted to an equivalent OD of 2.5×10^{-5} and grown in the cell counting device. Measurements are acquired during 3 min and subsequently averaged over 18 min; grey area shows the SEM. Different grey levels show independent replicates, and have been slightly time shifted to account for small differences in lag duration. According to Fig. 3(a), 1 AU corresponds to $\sim 1.0 \times 10^8$ ml^{-1}. (b) Growth of yeast *S. cerevisiae* S288C in YNB supplemented with 4 mM glucose and 4 mM fructose at 30 °C. Stationary phase culture are washed and diluted to an equivalent OD of 5×10^{-5} and grown in the cell counting device. Measurements are acquired during 3 min and subsequently averaged over 55 min; grey area shows the SEM. Different grey levels show independent replicates. According to Fig. 3(b), 1 AU corresponds to $\sim 3.0 \times 10^7$ ml^{-1}.

Studying microbial populations in growth media with low nutrient concentrations has always been challenging since the limited resources generally constrain the population size below the detection threshold of photometric methods. Here, we study the growth of *S. cerevisiae* in a low concentration glucose + fructose environment (4 mM each) starting with diluted populations (~ 500 ml^{-1}). We observe a long lag phase (almost 10 h) followed by exponential growth and stationary phase (Fig. 4(b)). The exponential growth is not limited by the interactions inside the population but by nutrient availability.

D. Fluorescence-based concentrations measurements

In order to study mixed populations, the ability to distinguish cells based on their fluorescence is a valuable tool. To assess the use of fluorescence intensity fluctuations (FIF) in exactly the same way as done for FIS, we compare in the following the estimation of the population density of fluorescent bacteria using simultaneously FIS and FIF. We study pure cultures of *E. coli* heat-killed (1 h at 70 °C) and stained with propidium iodide (PI), a DNA intercalating agent that preferentially stains cells with permeabilized membranes.[23] In these conditions, almost all the population is fluorescent. Using the dual-view feature of our setup, we can acquire on the same camera both the scattered and fluorescent light. Due to the higher intensity of the scattered light, we attenuated it by a factor of 20 (using a 1.3 neutral density filter; Fig. 5(a)) in order to match the camera sensitivity in the two channels. Because of the lower level of the fluorescence signal, we also required to increase the illumination intensity to ∼10 mW as well as the camera exposure time and gain so as to use most of the dynamic range of the camera.

As shown in Fig. 5, the concentration of the fluorescent population can be successfully estimated using FIF and within the same range of concentrations (10^4 ml^{-1}–10^8 ml^{-1}) as when analyzing the fluctuations of the intensity of the scattered light (the FIS approach).

Satisfyingly, in absence of PI, i.e., without fluorescent bacteria, a null concentration is measured in the fluorescence channel while the FIS measurement yields values that are indistinguishable from the ones with PI (Fig. 5).

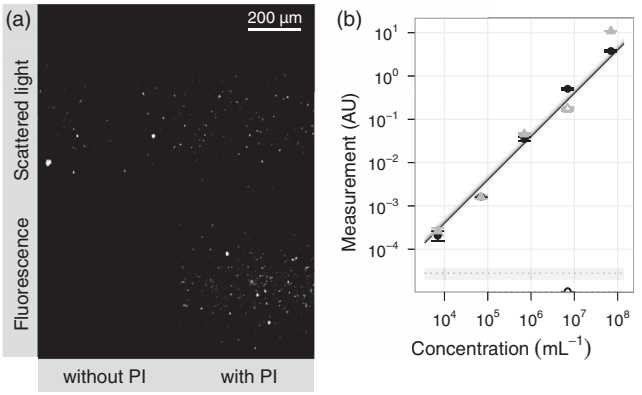

FIG. 5. Fluorescence-based microbial concentration measurements. Our counting method can be extended to the analysis of fluctuations in fluorescence intensity (instead of scattered light): *E. coli* cells are heat-killed and stained with PI. (a) Typical dual-view movie obtained with heat-killed *E. coli* at 7×10^6 mL^{-1} without (left) or with (right) PI. The upper beam corresponds to scattered light wavelength (below 550 nm) while the lower beam corresponds to fluorescence wavelength (above 550 nm). Acquisition frequency is 3.77 Hz and exposure time is 20 ms. Contrast has been adjusted to improve particle visibility. Scale bar is 200 μm (enhanced online) [URL: http://dx.doi.org/10.1063/1.4729796.2]. (b) Fluorescence-based measurements are shown with black circles and values measured after scattered light are plotted with grey triangles for comparison (close symbols). Points and error bars are mean and SEM of ten repeated measurements (seven in the case of fluorescence due to probe bleaching), dashed lines and greyed areas indicate the background level measured with a magnesium sulfate solution (undistinguishable from 0 in the case of fluorescence). The solid lines show linear fits with slope fixed to 1. Open symbols show measurements without PI for the 7×10^6 ml^{-1} sample (fluorescence channel yields 0).

To conclude, our method allows us to estimate the concentration of fluorescent microbial cells. As it measures fluorescent intensity fluctuations, this approach is likely to be more reproducible than simple fluorometric measurements which are sensitive to variations in the average background fluorescence between samples. Importantly, our approach opens the way to the study of mixed microbial populations, for instance, by measuring the ratio of the concentration of fluorescent cells to the total concentration (measured using FIS).

V. CONCLUSIONS

We have described a new and simple method for the measurement of microbial concentrations. This method works well across a wide range of concentrations and in particular at low concentrations, from 10^3 ml^{-1} to 10^8 ml^{-1}. This extends by more than two orders of magnitude of the range of classical OD measurements. Although the method requires an initial calibration, it does not require sampling and is thus very well suited for continuous monitoring of microbial growth. Moreover, it can be extended to the identification of two subpopulations with different fluorescence properties.

Other non-flowing laser light scattering methods have already been proposed, in particular to study blood samples (see, for instance, Yang *et al.*[24]). Although these methods allow one to distinguish between different cell types, they usually span a very limited range of concentrations (less than one order of magnitude).

When compared with the recently proposed digital in-line holographic microscopy approach, our method has a comparable dynamic range, acquisition duration, and cost: the choice to use one rather than the other will depend on experimental requirements. In particular, digital in-line holographic microscopy allows one to determine microbial position. Nonetheless, our method is easier to implement and much less computer intensive. Importantly, it can also be extended to distinguish species with different fluorescence properties. From a performance viewpoint, it is difficult to compare the accuracy of the estimation obtained with the two methods as the calibration plot given by Frentz *et al.*[19] spans a much narrower range of concentrations.

Finally, an important challenge of microbial ecology is the study of population dynamics in spatially structured environments.[25] In particular, the detection of colonization events in empty niches requires good sensitivity at low concentration. Using our method, it is possible to scan the sample (either by displacing the beam or by moving the sample) instead of relying on convection (or stirring) of the cells to acquire independent images. Consequently, our method can easily be extended to the study of microbial populations in spatially structured environments.

ACKNOWLEDGMENTS

We are grateful to John Koschwanez and Andrew Murray for providing strains and advice for the experiments

with yeast. We thank Gordon Hamilton and one anonymous referee for their valuable comments on the manuscript.

[1]F. K. Balagaddé, H. Song, J. Ozaki, C. H. Collins, M. Barnet, F. H. Arnold, S. R. Quake, and L. You, Mol. Syst. Biol. **4**, 187 (2008).
[2]M. Varon and B. P. Zeigler, Appl. Environ. Microbiol. **36**, 11 (1978).
[3]E. Chi Fru, I. D. Ofiţeru, V. Lavric, and D. W. Graham, Appl. Microbiol. Biotechnol. **89**, 791 (2011).
[4]K. R. Foster, Nat. Rev. Genet. **12**, 193 (2011).
[5]S. Elena and R. Lenski, Nat. Rev. Genet. **4**, 457 (2003).
[6]A. Eldar, V. K. Chary, P. Xenopoulos, M. E. Fontes, O. C. Losón, J. Dworkin, P. J. Piggot, and M. B. Elowitz, Nature (London) **460**, 510 (2009).
[7]C. M. Jessup, S. E. Forde, and B. J. Bohannan, in *Population Dynamics and Laboratory Ecology*, Advances in Ecological Research, Vol. 37 (Academic, 2005), pp. 273–307.
[8]G. S. Wilson, J. Bacteriol. **7**, 405 (1922).
[9]R. Smither, J. Appl. Bacteriol. **39**, 157 (1975).
[10]E. M. Swanton, W. A. Curby, and H. E. Lind, Appl. Environ. Microbiol. **10**, 480 (1962).
[11]T. E. Shehata and A. G. Marr, J. Bacteriol. **107**, 210 (1971).
[12]T. S. Gunasekera, P. V. Attfield, and D. A. Veal, Appl. Environ. Microbiol. **66**, 1228 (2000).
[13]F. Hammes, M. Berney, Y. Wang, M. Vital, O. Köster, and T. Egli, Water Res. **42**, 269 (2008).
[14]A. L. Koch, Biochim. Biophys. Acta **51**, 429 (1961).
[15]T. Fujita and K. Nunomura, Appl. Microbiol. **16**, 212 (1968).
[16]P. O. Byrne, T. S. J. Elliott, P. R. Sisson, P. D. Oliver, and H. R. Ingham, J. Phys. E **22**, 146 (1989).
[17]M. Novak, T. Pfeiffer, M. Ackermann, and S. Bonhoeffer, Antonie Van Leeuwenhoek **96**, 267 (2009).
[18]E. Dekel and U. Alon, Nature (London) **436**, 588 (2005).
[19]Z. Frentz, S. Kuehn, D. Hekstra, and S. Leibler, Rev. Sci. Instrum. **81**, 084301 (2010).
[20]See supplementary material at http://dx.doi.org/10.1063/1.4729796 for supplementary table and figures.
[21]P. Kask, K. Palo, D. Ullmann, and K. Gall, Proc. Natl. Acad. Sci. U.S.A. **96**, 13756 (1999).
[22]A. Katz, A. Alimova, M. Xu, E. Rudolph, M. Shah, H. Savage, R. Rosen, S. McCormick, and R. Alfano, IEEE J. Sel. Top. Quantum Electron. **9**, 277 (2003).
[23]R. López-Amorós, S. Castel, J. Comas-Riu, and J. Vives-Rego, Cytometry **29**, 298 (1997).
[24]Y. Yang, Z. Zhang, X. Yang, J. H. Yeo, L. Jiang, and D. Jiang, J. Biomed. Opt. **9**, 995 (2004).
[25]P. B. Rainey and M. Travisano, Nature (London) **394**, 69 (1998).